Korean J. Chem. Eng., 35(1), 263-271 (2018)
DOI: 10.1007/s11814-017-0249-0

pISSN: 0256-1115
eISSN: 1975-7220

Effect of assembly condition on the morphologies and temperature-triggered transformation of layer-by-layer microtubes

Choonghyun Sung*,† and Jodie L. Lutkenhaus**

*Polymeric Materials Engineering Major, Division of Advanced Materials Engineering, Dong-Eui University, Busan 47340, Korea
**Artie McFerrin Department of Chemical Engineering, Texas A&M University, College Station, Texas 77843, United States
(*Received 27 July 2017 • accepted 13 September 2017*)

Abstract−The morphology and temperature-triggered transformation of the LbL microtubes consisting of poly(allylamine hydrochloride) (PAH) and poly(acrylic acid) (PAA) were investigated as a function of assembly pH, polyelectrolyte molecular weight (MW), and multivalent ions. The as-made microtubes assembled at pH 5.5 (PAH)/5.5 (PAA) showed perforations on the surface, while those assembled at pH 7.5 (PAH)/3.5 (PAA) showed smooth surface without perforations. At the same MW, the microtubes assembled at pH 7.5/3.5 transformed more effectively compared to those assembled at pH 5.5/5.5. The aspect ratio of microtubes assembled at pH 7.5/3.5 decreased from 5 to 2 as the temperature increased from room temperature to 121 °C. Furthermore, transformation of microtubes was facilitated as the MW of polyelectrolytes decreased. The dimensional stability of microtubes was influenced by the MW and added multivalent ions. These results were discussed in the context of the structure of the LbL assemblies.

Keywords: Layer-by-layer, Transformation, Microtube, Assembly pH, Molecular Weight

INTRODUCTION

Layer-by-layer (LbL) assembly is a simple and versatile nanofabrication technique to build polyelectrolyte multilayers [1]. Various substrates are exposed to oppositely charged polyelectrolyte solutions with the rinsing steps in-between. Film growth, structure, and properties of LbL assemblies can be fine-tuned by varying polymer composition and assembly conditions such as pH and salt concentration [2,3]. Furthermore, inorganic or metallic nanoparticles are easily incorporated into LbL assemblies [4,5].

Structured LbL assemblies such as hollow capsules and microtubes have attracted considerable interest [6,7]. They have found a variety of applications in drug delivery, biosensors, nanoreactor, and photovoltaics. Structured LbL assemblies are frequently prepared by template-assisted fabrication methods [8]. Polyelectrolyte multilayers are deposited on a template such as spherical particles or porous membranes. Then, microcapsules or LbL microtubes are released upon the removal of templates.

LbL microcapsules have been extensively studied especially for the application of drug delivery and life science [6,9,10]. Therefore, the behavior of LbL microcapsules in aqueous solution is of considerable interest. LbL microcapsules of poly(diallyldimethylammonium chloride) (PDADMA)/poly(styrene sulfonate) (PSS) exhibited intriguing behavior upon heating in aqueous media [11-13]. PDADMA/PSS microcapsules with PSS as the outermost layer showed pronounced shrinkage upon heating at 70 °C for 20 min, whereas the microcapsules with PDADMA as the outermost layer swelled significantly until they ruptured at 55 °C [12]. Recently, the shrinkage properties of PDADMA/PSS capsules have been used for drug delivery applications [14,15]. On the other hand, PAH/PSS microcapsules showed shrinkage regardless of the identity of the outermost layer [16-18]. PAH/PSS microcapsules shrank less than one-third of their initial size upon incubating at 120 °C for 20 min [17], while shrinkage was negligible at 70 °C for 2 hr [16]. This thermal behavior has been explained with regard to a thermal transition [13]. Electrostatic forces cause swelling and hydrophobic forces cause shrinkage in the hollow capsule. Above the thermal transition temperature, the rearrangement of polymer chains is facilitated, and microcapsules either shrink or swell depending on the force balance influenced by the outermost layer.

The above thermal behavior of microcapsules has triggered interest in the thermal transitions of LbL assemblies. Various methods such as modulated differential scanning calorimetry (DSC) [19], micro DSC [13], nuclear magnetic resonance spectroscopy [20], and quartz crystal microbalance with dissipation [21] have been used to study the thermal transition temperature (T_{tr}). T_{tr} can be categorized into T_{tr}'s for dry and hydrated LbL systems. For electrostatic LbL assemblies, T_{tr} has been reported only in hydrated states [13,20-22]. PDADMA/PSS LbL films showed thermal transitions with the addition of salts [21,23]. QCM-D studies of LbL assemblies of PAH and poly(acrylic acid) (PAA) showed that hydrated PAH/PAA LbL assemblies undergo a thermal transition for most assembly pH values with the exception where both polyelectrolytes are fully charged [22].

Early studies postulated that the thermal transition arose owing to the partial dissociation of ion-paring of polyelectrolytes in aque-

†To whom correspondence should be addressed.
E-mail: chsung@deu.ac.kr

ous solution. QCM-D studies of PDADMA/PSS LbL films demonstrated that the thermal transition was associated with a minor flux of water into and out of the LbL film [21]. Differentiating from the conventional glass transition temperature, T_{tr} for LbL films has been called a glass-melt transition temperature (T_{gm}) in LbL communities. Recently, studies on the nature of the thermal transitions of polyelectrolyte complexes, which gives insight for LbL films, have been published. Molecular simulations of PDADMA/PSS polyelectrolyte complexes identified the important role of water in thermal transition. It was demonstrated that the thermal transition was accompanied by a decrease in the water-polyelectrolyte hydrogen bond lifetime [24,25]. Extending the studies, the effect of water on the PAH/PAA complex was also studied using modulated DSC [26]. Zhang et al. showed that all T_{tr} values sit on a single master curve when plotted against the ratio of water molecules per intrinsic PAH/PAA ion pair for all complexation pH values. The T_{tr} value decreased as the ratio of water molecules per intrinsic PAH/PAA ion pair increased. It was proposed that the thermal transition is accompanied by increased dynamics of water molecules near the intrinsic PAH/PAA ion pair in the water-polyelectrolyte hydrogen bonding network, followed by chain relaxation. Thus, instead of the glass-melt transition, the term thermal transition temperature (T_{tr}) is used in this paper.

Compared to LbL microcapsules, there are only a handful of studies on the thermal behavior of LbL microtubes in aqueous solution. He et al. reported the transformation of PAH/PSS nanotubes after incubation at 121 °C for 20 min [27]. The outer diameter of 400 nm PAH/PAA nanotubes transformed to 500 nm-1 μm diameter spheres or hollow capsules. However, the thermal behavior of PAH/PAA nanotubes was studied at a fixed temperature of 121 °C [27]. Recently, we investigated temperature-triggered transformations in shape of PAH/PAA LbL microtubes in aqueous solution [28]. PAH/PAA LbL microtubes were prepared by assembling LbL films in the cylindrical pores of PC membranes. When the released LbL microtubes were incubated at high temperatures, the microtubes transformed to ellipsoidal shapes. On the other hand, unreleased LbL microtubes, attached to the pores of a membranes, showed periodical perforations on the microtube surface, indicative of Rayleigh instabilities. However, the authors focused their study on the microtubes prepared at single assembly condition, pH of 7.5 and 3.5 for PAH and PAA, respectively.

Here, extending the previous study, we studied the effect of assembly pH, molecular weight (MW), and multivalent ions on the morphology and temperature-triggered transformation of PAH/PAA microtubes. Assembly pH is important parameter for LbL assemblies of weak polyelectrolytes such as PAH and PAA used in this study. MW and multivalent ions are also important parameters that control the growth and interpenetration. Results are discussed based on structure of PAH/PAA LbL films.

EXPERIMENTAL

1. Materials

Poly(allylamine hydrochloride) (PAH) of three different MW's, 15,000 g/mol, 58,000 g/mol, and 160,000 g/mol, were purchased from Sigma Aldrich. Poly(acrylic acid)(PAA) of two MW's, 50,000 g/mol, and 100,000 g/mol, were also obtained from Sigma Aldrich. Track-etched polycarbonate (PC) membranes (Nucleopore™) were purchased from Whatman. The cylindrical pore diameter and thickness were 1 μm and 10 μm, respectively. Three combinations of MW's were used for the assembly of LbL film: low MW (PAH 15,000 g/mol, PAA 50,000 g/mol), medium MW (PAH 58,000 g/mol, PAA 50,000 g/mol), and high MW (PAH 160,000 g/mol, PAA 100,000 g/mol).

2. Deposition of LbL Film

LbL microtubes were prepared using a PC membrane as a porous template. LbL films were deposited in the cylindrical pores of the PC membrane using a programmable slide stainer. PC membranes were immersed in 10 mM PAH solution for 15 min followed by three consecutive rinses in DI water for 2 min, 1 min, and 1 min. Then, the PAH-coated PC membranes were immersed in 10 mM PAA solution for 15 min, followed by another three rinses in DI water in the same protocol as before. This polyelectrolyte coating process was repeated to yield n layer pairs, denoted as $(PAH/PAA)_n$. Assembly pH was adjusted using dilute NaOH and HCl. LbL film-coated membrane samples were dried overnight at room temperature. Two assembly pH conditions were used in this study. One is pH 5.5 for both PAH and PAA, while the other is pH 7.5 and pH 3.5 for PAH and PAA, respectively. The former condition is denoted as pH 5.5/5.5 and the latter is denoted as pH 7.5/3.5 hereafter.

3. Preparation and High Temperature Incubation of LbL Microtubes

After LbL films were coated on the pores of PC membranes, LbL microtubes were released by dissolving the PC membrane templates. Prior to the dissolution of PC membranes, each side of the LbL film-coated PC membranes was plasma-etched for 10 min to remove excess polymer film from the membrane surface. PAH/PAA LbL microtubes were released by the selective dissolution of the PC membranes using dichloromethane (DCM). Then LbL microtubes were washed by centrifugation at 7,000 rpm for 10 min followed by re-dispersion in fresh dichloromethane for three cycles. LbL microtubes were washed with ethanol twice using the same protocol and re-dispersed in DI water at pH 5.5. The microtubes-in-water suspensions were incubated in a temperature-controlled water bath for various temperatures. All samples were sonicated for 3 min right before incubation. For incubation at 121 °C, an autoclave (Steris, Amsco Lab 250) was used. A schematic diagram of the preparation and hydrothermal treatment of LbL microtubes is shown in Fig. 1.

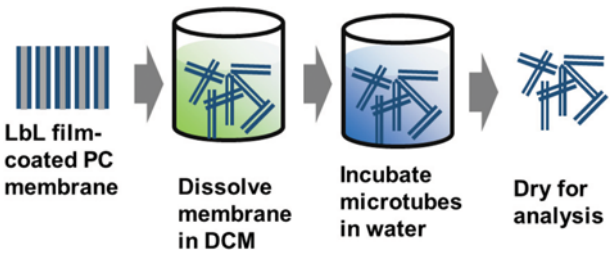

Fig. 1. A schematic illustration of preparation and incubation of LbL microtubes.

4. Electron Microscopy

Scanning electron microscopy (SEM) images were obtained using JEOL JSM-7500F or FEI Quanta 600. A few drops of LbL microtube suspension were cast onto silicon water and dried overnight at room temperature. The dried samples were then sputtered with ~7 nm thick Pt for SEM observation. Transmission electron microscopy (TEM) images were collected using a JEOL 1200 EX operating at a voltage of 100 kV. The suspensions were cast and dried on the carbon-coated copper grids.

To observe the morphology of LbL microtubes before the incubation, the samples dried from LbL microtubes-in-dichloromethane suspension were used. To observe the morphology changes of in aqueous solutions, images of LbL microtubes, dried from aqueous solution after the high temperature incubation, were obtained. If desired, the length and the outer diameter of at least 30 microtubes were measured from SEM images, and the results were averaged.

RESULTS

1. Morphologies of As-made LbL Microtubes

First, we explored the LbL microtubes assembled at pH 5.5/5.5. Fig. 2 shows the effect of LbL assembly condition on the morphologies of LbL microtubes prepared using low MW PAH (15,000 g/mol) and PAA (50,000 g/mol) was investigated. SEM images of $(PAH/PAA)_{17}$ LbL microtubes were taken after the dissolution of PC membrane in DCM. Comparing Fig. 2(a) and 2(b), the absence of sonication during the PC membrane dissolution is critical for the preservation of microtube shape. Sonication was applied to dissolve the PC membrane effectively and to separate the individual microtubes. However, it seems LbL microtubes prepared in this condition are so brittle that gentle sonication is strong enough to break the LbL microtubes (Fig. 2(a)). In contrast, sonication does not damage the microtubes in water. When microtubes are re-dispersed in an aqueous solution, the microtubes are hydrated and become soft. Thus, microtubes do not break in aqueous solution by sonication.

Although the LbL microtube shape is maintained in the absence of sonication, perforations are exhibited in the microtubes (Fig. 2(b)). To minimize the perforation, we increased the dipping time from 15 min to 30 min allowing sufficient time for the polymer chains to diffuse into the pores of PC membranes. However, the perforations did not diminish as shown in Fig. 2(c). We also applied poly(ethylene imine) as an adhesion promoter prior to the deposition of PAH and PAA, but it was not effective for removing perforations. The perforations were weakened when the surfaces of the PC carbonate membrane were cleaned with Kimwipes every four layer pair (LP) and the number of the LP was increased to 26 (Fig. 2(d)). It seems the intermittent cleaning removes the polymer aggregates on the pore entrance and more polymer chains fill the perforations as the LP (i.e., film thickness) increases. The thickness of 26 LP was ~500 nm on silicon substrate while the thickness on the pores of PC membrane was about 100 nm at the same 26 LP. Thus, LbL deposition on the PC membrane pore is more challenging.

When multivalent ions are added to polyelectrolyte solution, polyelectrolytes shrink due to the ion-bringing effect [29]. The Char group showed that polymer chains could diffuse into pores

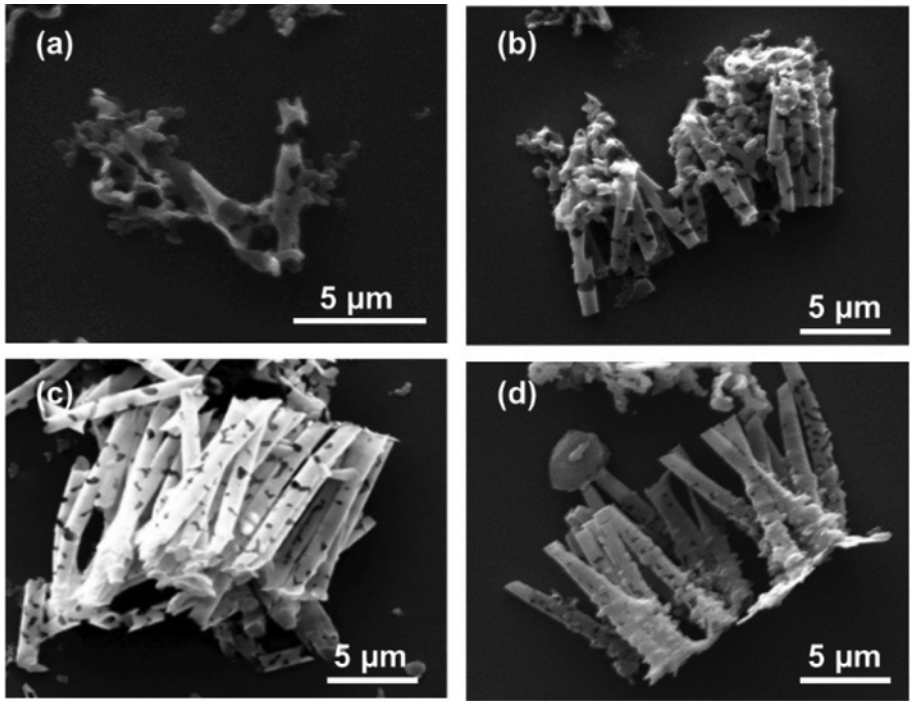

Fig. 2. SEM images of $(PAH/PAA)_{17}$ LbL microtubes with (a) dipping 15 min, sonication 5 min (b) dipping 15 min, sonication 0 min (c) dipping 30 min, sonication 0 min. SEM images of (d) $(PAH/PAA)_{26}$ LbL microtubes with dipping 15 min, sonication 0 min, cleaning every 4 LP. MW of PAH and PAA is 15,000 g/mol and 50,000 g/mol, respectively. Assembly pH is 5.5/5.5 for all conditions.

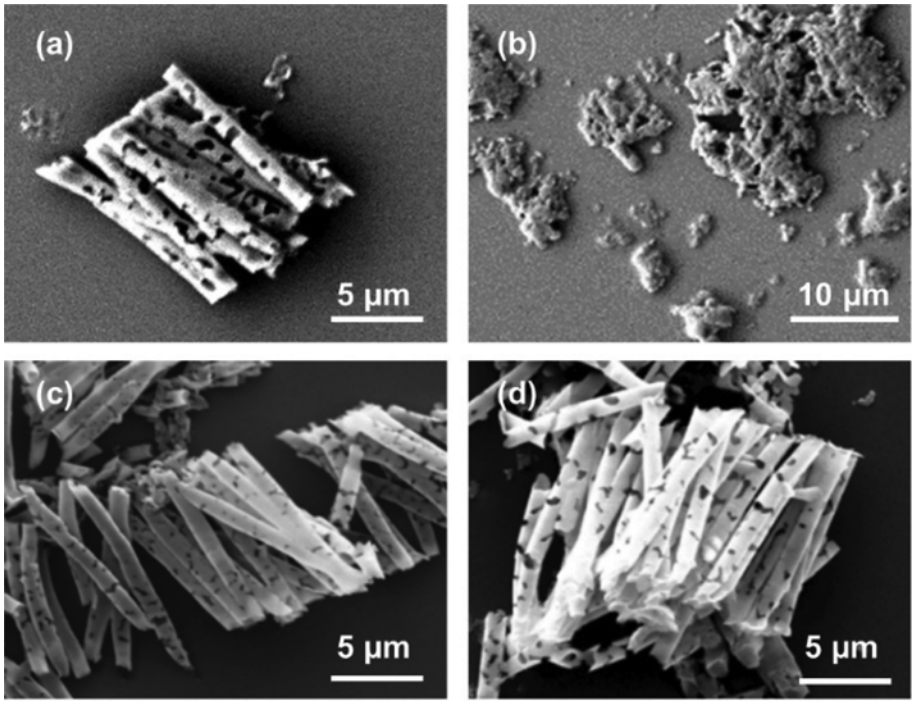

Fig. 3. SEM images of $(PAH/PAA)_{19}$ LbL microtubes assembled at pH 5.5/5.5 with (a), (b) PAH 15,000 g/mol, PAA 50,000 g/mol, $CaCl_2$ 2 mM (c) PAH 160,000 g/mol, PAA 100,000 g/mol, $CaCl_2$ 2 mM (d) PAH 58,000 g/mol, PAA 50,000 g/mol, no $CaCl_2$. Fig. 3(a), (c), (d) were dried from dichloromethane and Fig. 3(b) were dried from the aqueous solution at room temperature.

of a anodic aluminum oxide membrane more easily below $CaCl_2$ concentration of 5 mM [30]. In our study, $CaCl_2$ of 2 mM was added to the both polyelectrolyte solutions as it might reduce the perforations in the LbL microtubes. However, when $CaCl_2$ was added to the solution of PAH (15,000 g/mol) and PAA (50,000 g/mol), we could not see improvement in the reduction of perforations (Fig. 3(a)). It implies that the conformation of polyelectrolyte is not a critical factor for the occurrence of the perforations. Furthermore, when the microtubes were re-dispersed in water and dried, most of the microtubes melted or disintegrated (Fig. 3(b)). We also used high MW PAH (160,000 g/mol) and PAA (100,000 g/mol). In our preliminary study, when PAH and PAA of these high MWs were used, many pores were not effectively coated, indicating that diffusion through the pores is deterred due to the high MW of polyelectrolytes. Thus, we added $CaCl_2$ to high MW PAH and PAA solution. In this assembly condition, the microtubes maintained the dimensional integrity but still showed perforations (Fig. 3(c)). When re-dispersed in water and dried, the microtubes did not melt or disintegrated in contrast to those prepared from the low MW PAH and PAA. The LbL microtubes were also prepared using medium MW PAH (58,000 g/mol) and PAA (50,000 g/mol) (Fig. 3(d)). The microtubes at these conditions also showed perforations on the microtubes. The microtubes, both prepared from medium and high MW PAH and PAA, showed some perforations even though the membrane surface was cleaned with Kim wipes every four bilayers and released without sonication. Furthermore, the microtubes prepared from medium and high molecular weight PAH and PAA did not break even though sonication was applied in dichloromethane for membrane dissolution. Of note, the wall thickness of $(PAH/PAA)_{19}$ for both low and medium MW PAH and PAA was about 130 nm.

The microtubes were also prepared at assembly pH of 7.5/3.5 for PAH and PAA, respectively. This is the pH condition where PAH and PAA are less ionized and have less extended chain conformation. At this pH condition, perforations are not observed regardless of polymer MW, as shown in Fig. 4. In this case, neither intermittent cleaning with wipes nor addition of $CaCl_2$ was required. Even though we applied sonication in DCM solution for the dispersion of microtubes, the microtubes did not break (Fig. 2(a) vs. Fig. 4). The microtubes assembled using both low MW PAH (15,000 g/mol) and PAA (50,000 g/mol) (Fig. 4(a)), and medium MW PAH (58,000 g/mol) and PAA (50,000 g/mol) (Fig. 4(b)), showed a smooth surface without perforations. Wall thickness of microtubes assembled with medium MW was about 110 nm as obtained from TEM imaging (Fig. 4(d)).

2. Effect of Thermal Incubation on the Transformation of LbL Microtubes

The microtubes were released from PC membranes by dissolving in the dichloromethane followed by washing with ethanol and re-dispersing in water at pH 5.5. Then, the microtubes-in-water suspensions were incubated at high temperatures. Fig. 5 shows the SEM images of microtubes assembled at pH 5.5/5.5 before and after incubation at 121 °C. The microtubes dried from water without high temperature incubation (Fig. 5(a)-(d)) show different morphologies compared to the microtubes (Fig. 2 and 3) dried from dichloromethane to release from the membrane. The microtubes dried from dichloromethane reflect the exact dimension of cylindrical pores and show a smooth surface. In contrast, the micro-

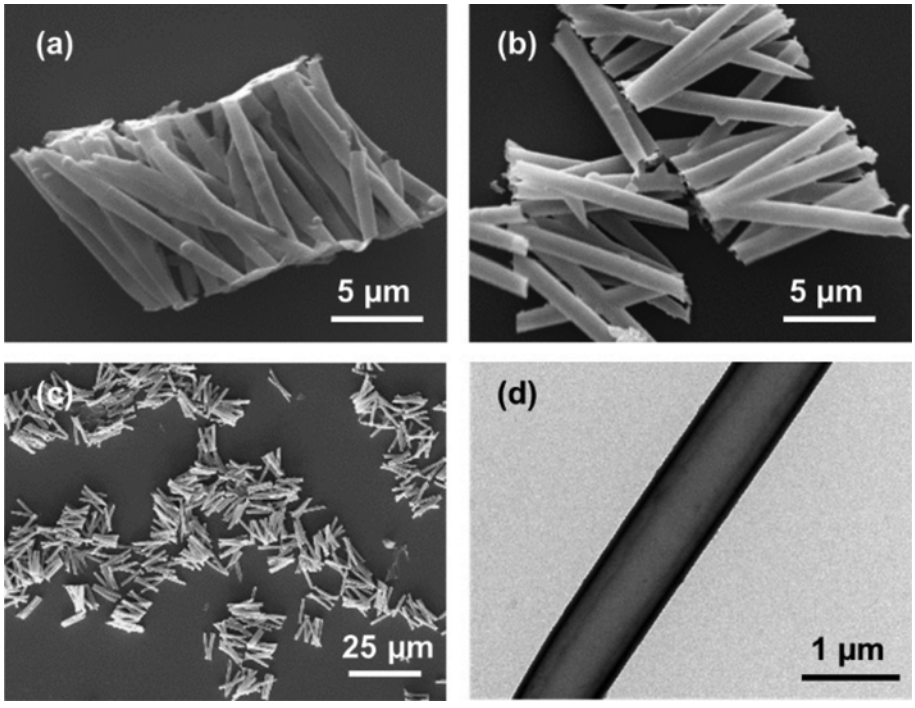

Fig. 4. SEM and TEM images of $(PAH/PAA)_{10}$ microtubes assembled at pH 7.5/3.5 with (a) PAH 15,000 g/mol and PAA 50,000 g/mol, (b), (c), (d) PAH 58,000 g/mol and PAA 50,000 g/mol.

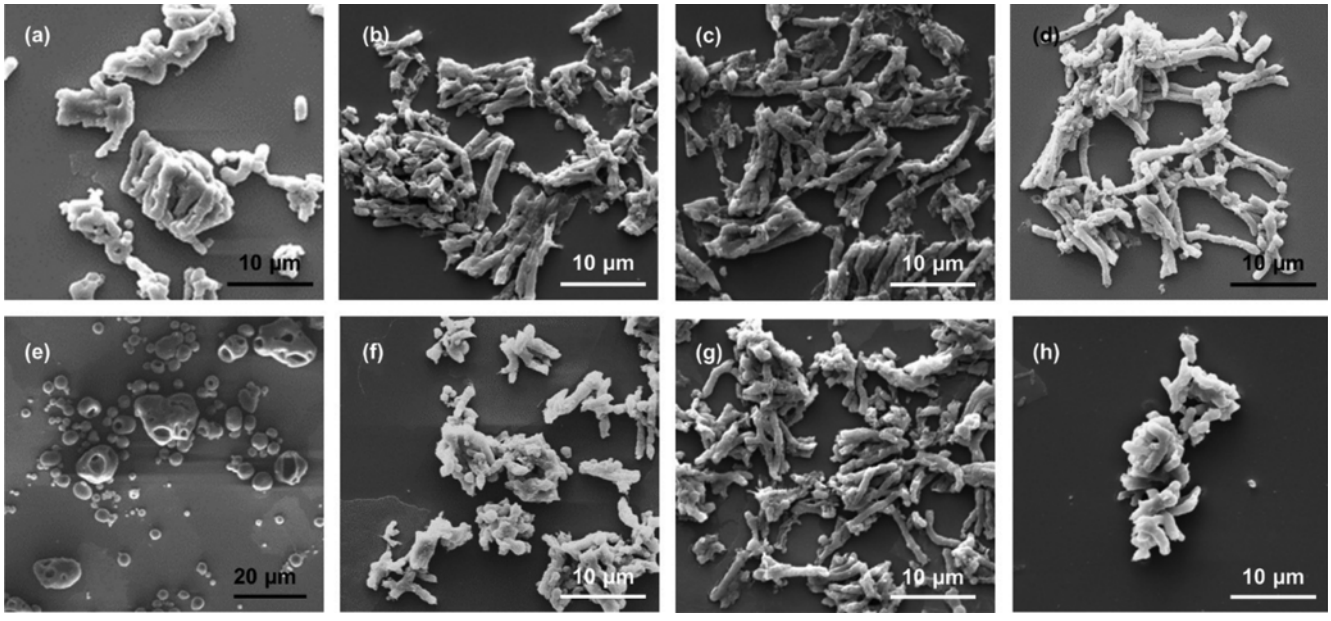

Fig. 5. SEM images LbL microtubes of (a), (e) PAH 15,000 g/mol PAA 50,000 g/mol, 26 LP, (b), (f) PAH 58,000 g/mol PAA 50,000 g/mol, 19 LP. SEM images of microtubes of PAH 160,000 g/mol PAA 100,000 g/mol for (c), (g) 19 LP (d), (h) 11 LP. Fig. 5(a), (b), (c), (d) and Fig. 5(e), (f), (g), (h) are the images of microtubes before and after thermal incubation, respectively. Assembly pH is 5.5/5.5 for all the conditions.

tubes dried from water show very curved and deformed shapes. The surface of the microtubes is rough and the diameter of the microtubes is inconsistent. Also, perforations on the microtubes seem to have disappeared or closed upon hydration. The transformation of LbL microtubes at high temperature was also investigated (Fig. 5(e)-(h)). Transformation effectiveness seems to be influenced by the MW's of PAH and PAA. When the MW's were lowest (PAH 15,000 g/mol, PAA 50,000 g/mol), the microtubes transformed into ellipsoidal shapes as shown in Fig. 5(e). The diameter of the ellipsoids was 2-5 μm, except for big agglomerates. In con-

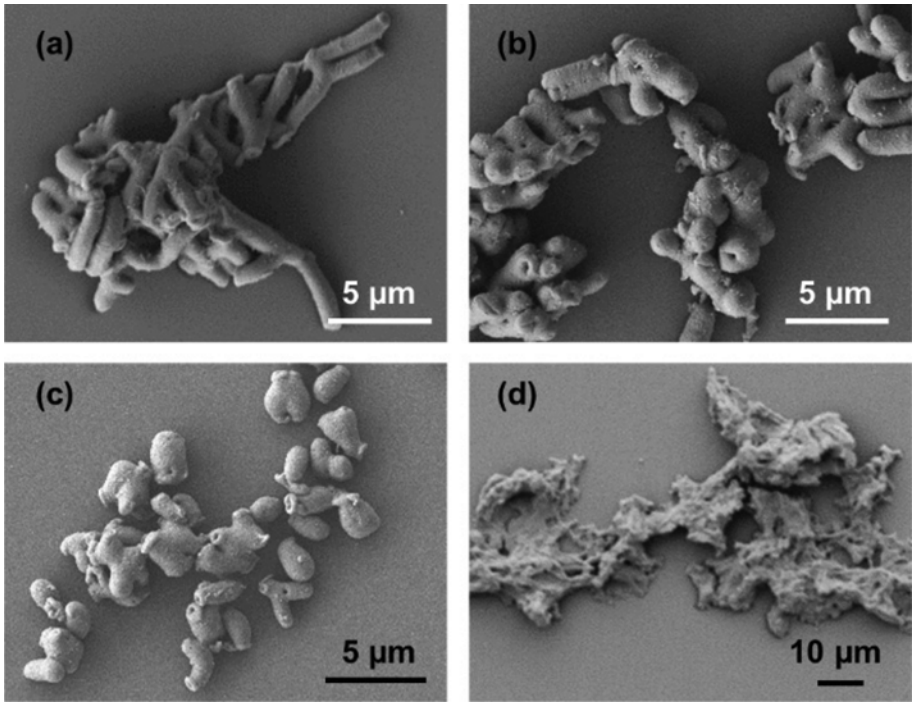

Fig. 6. SEM images of $(PAH/PAA)_{10}$ LbL microtubes assembled with medium MW PAH (58,000 g/mol) and PAA (50,000 g/mol) incubated in water at (a) 25 °C, (b) 70 °C, and (c) 121 °C. (d) SEM images of $(PAH/PAA)_{10}$ LbL microtubes assembled with low MW PAH (15,000 g/mol) and PAA (50,000 g/mol) incubated at 25 °C. Assembly pH is 5.5/5.5 for all the conditions.

trast, when the MW's of PAH and PAA were higher, LbL microtubes were not effectively transformed into ellipsoidal shapes. The microtubes assembled with medium MW PAH (58,000 g/mol) and PAA (50,000 g/mol) showed noticeable contraction (Fig. 5(f)), while those assembled with high MW PAH and PAA, of similar wall thickness, showed negligible transformation (Fig. 5(g)). The number of LPs is another factor influencing the shape transformation. For LbL microtubes assembled with high MW PAH (160,000 g/mol) and PAA (100,000 g/mol) along with added $CaCl_2$, LbL microtubes contracted roughly 40% when the LP value decreased from 19 to 11, Fig. 5(h). Of note, it was impossible to quantitatively measure the length and diameter of the microtubes due to the irregular shape of microtubes.

Next, transformation of LbL microtubes prepared at pH values of 7.5/3.5 was investigated (Fig. 6). In contrast to the LbL microtubes assembled at pH 5.5/5.5, the surface of microtubes assembled with MW's of PAH (58,000 g/mol) and PAA (50,000 g/mol) were smooth and the dimension was quite consistent before high temperature incubation (Fig. 6(a)). As the incubation temperature increased from 70 °C to 120 °C, contraction of the LbL microtubes increased (Fig. 6(b) and 6(c)). However, when the MW's of PAH (15,000 g/mol) and PAA (50,000 g/mol) were low for assembly pH 7.5/3.5, the microtubes melted in aqueous solution (Fig. 6(d)), in contrast to the microtubes assembled at pH 5.5/5.5 with the same MW PAH and PAA (Fig. 5(a)). Of note, the microtubes assembled at pH 5.5/5.5 with $CaCl_2$ melted and aggregate together upon drying from the dichloromethane, prior to dispersion in water (Fig. 3(b)).

The transformation of LbL microtubes prepared at pH 7.5/3.5 with medium MW PAH (58,000 g/mol) and PAA (50,000 g/mol) was investigated at varying incubation temperatures. Fig. 6(b) and 6(c) show the SEM images of the microtubes incubated at 70 °C for 1 hr and 121 °C for 45 min, respectively. The length decreased and the diameter increased as the incubation temperature increased. To quantify the transformation against temperature, the length and diameter of LbL microtubes were measured from SEM images of microtubes incubated at varying temperatures. Fig. 7 shows the aspect ratio of length and diameter of LbL microtubes as a func-

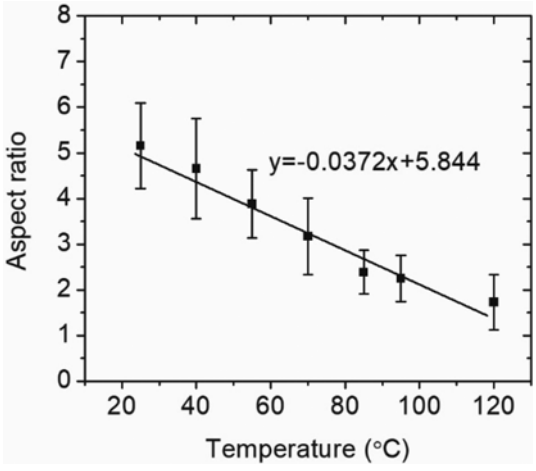

Fig. 7. The aspect ratio of length and diameter of $(PAH/PAA)_{10}$ LbL microtubes as a function of incubation temperature. Assembly pH is 7.5/3.5 and MW of PAH and PAA is 58,000 g/mol and 50,000 g/mol, respectively.

tion of incubation temperature. As the incubation temperature increased from room temperature to 121 °C, the aspect ratio decreased fairly linearly from 5 to 2. Although the hydrated PAH/PAA LbL films assembled at pH 7.5/3.5 exhibited hydrated thermal transition temperature at ~71 °C as measured by MDSC [28], no clear transition or discontinuity was observed in the plot of aspect ratio vs. incubation temperature.

DISCUSSION

The microtubes assembled at pH 5.5/5.5 and 7.5/3.5 with medium MW PAH (58,000 g/mol) and PAA (50,000 g/mol) show different morphologies. While the as-made microtubes assembled at pH 5.5/5.5 show perforations on the surface, the microtubes assembled at pH 7.5/3.5 show a smooth surface without perforations. At assembly pH 5.5/5.5, PAH is nearly fully charged and PAA is fully charged. In contrast, at assembly pH 7.5/3.5, PAH is nearly fully charged, and PAA is weakly ionized [31,32]. At pH 7.5/3.5, where PAA is weakly ionized, LbL films grow homogeneously in the membrane pores. On the other hand, at pH 5.5/5.5, where PAA is fully charged, we observe perforations on the film, which is the indication of inhomogeneous film growth. We think that the perforations are due to the ineffective wetting associated with the higher degree of ionization of PAA. PC membranes are relatively hydrophobic, and LbL films do not grow efficiently on the hydrophobic surfaces when both PAH and PAA are nearly fully charged. Liu et al. studied the film growth and the surface morphologies of PAH/PAA LbL films on a hydrophobic surface and a hydrophobic surface modified with cationic surfactant using high and low MW polyelectrolytes [33]. When the MW was high, LbL films grew readily on the cationic surface and showed limited growth on the hydrophobic surface. Furthermore, the LbL films grown on the cationic surface were relatively flat while the films grown on the hydrophobic surface beaded up. Based on these observations, it is possible that nearly fully charged PAH and PAA would form inhomogeneous films on the hydrophobic PC membrane, resulting in perforations in the LbL microtubes. When hydrophobic polystyrene solution dried inside the pores of hydrophilic anodic aluminum oxide [34], periodic perforations were also observed, which is indicative of Rayleigh instabilities [35]. It seems that LbL microtubes also generate perforations to reduce the interfacial energy.

Assembly pH is an important parameter controlling the structure and properties of PAH and PAA LbL films. The PAH/PAA LbL film assembled at pH 7.5/3.5 shows the highest layer thickness and roughness, manifested by many loops and tails [31]. Contact angles of these films depend upon the outermost layer, and the contact angles of LbL films with PAH and PAA outermost layers were 40° and 10°, respectively [31]. These results show that the surface of these films is dominated by the outermost polymer layer, implying relatively lower degree of interpenetration [31]. On the other hand, the LbL films assembled at pH 5.5/5.5 also have high layer thickness manifested from loops and tails. However, the contact angle of these films was approximately 25° regardless of the outermost layer, which means that PAH and PAA layers are highly interpenetrated [31]. From the porous transition studies of LbL films, it was identified that the PAH/PAA LbL films assembled at pH 5.5/5.5 did not swell, while the films assembled at pH 7.5/3.5 swelled three times the original thickness when the films were transferred from the aqueous solution of pH 5 to 2.5 [36]. These different swelling behaviors were exhibited despite both films having a similar degree of PAA ionization below pH 2.5. It was postulated that the films assembled at pH 5.5/5.5 might have "domains of cooperatively stitched chains [36]" within the intermingled structure, and these domains could act as crosslink points. In summary, the films assembled at pH 5.5/5.5 are more interpenetrated and possess more domains that act as crosslinking sites as compared to the films assembled at 7.5/3.5.

The dependence of dimensional stability of LbL microtubes in water is consistent with the above explanation. At the assembly condition of pH 7.5/3.5, the microtubes assembled with low MW PAH (15,000 g/mol) and PAA (50,000 g/mol) melted when dispersed in the water (Fig. 6(d)). In contrast, at the assembly pH 5.5/5.5, the microtubes assembled with low MW PAH and PAA roughly maintained the microtube shape (Fig. 5(a)). At pH 7.5/3.5, where interpenetration and ionic crosslink is lower, the microtubes seem to be destabilized due to the fewer entanglements among polymer chains as the MW's of PAH and PAA decreased. At pH 5.5/5.5 where interpenetration and ionic crosslinking is higher, the stability is better despite the low MW PAH and PAA. Transformation of microtubes is also influenced by the assembly pH in the same way. The microtubes assembled at pH 7.5/3.5 transformed into ellipsoidal shape more easily compared to those assembled at pH 5.5/5.5 at the same medium MW PAH and PAA (Fig. 5(b) vs Fig. 6). In summary, the films assembled at pH 5.5/5.5 show higher dimensional stability and less degree of transformation compared to the films assembled at pH 7.5/3.5 owing to the higher degree of interpenetration and domains of cooperatively stitched chains that act as crosslink points.

MW's of PAH and PAA influences the dimensional stability and transformation of microtubes. At pH 7.5/3.5, LbL microtubes assembled with medium MW PAH and PAA maintained the microtube shape, while those assembled with low MW melted in the water (Fig. 6(a) vs Fig. 6(d)). Minimum MW weight of PAH and PAA seems to be required for effective chain entanglements. Transformation is also affected by the MW and thickness of the microtubes. While the microtubes with low MW PAH and PAA assembled at pH 5.5/5.5 transform to ellipsoidal shape very easily (Fig. 5(a)), those with medium or high MW PAH and PAA showed less degree of transformation (Fig. 5(b) and 5(c)). We postulate that as the MW increases, the chain entanglement increases and mobility of polymer chains decreases, which hinders the rearrangement of polymer chains for the transformation. Also, the transformation became ineffective as the number of the layer pairs is increased from 11 LP to 19 LP (Fig. 5(c) and 5(d)). This is because the total number of the chains that need to be rearranged for transformation increases as more polymer layers are deposited. Also, it is possible that as more polymer layers are deposited, the degree of interpenetration, which deters transformation, increases.

Another explanation for the effect of MW on the transformation of the microtubes is associated with the number of ion-pairs per single polymer chain. As the MW of the polyelectrolyte de-

creases, the number of ion-pairs per single polymer chain in the film decreases. For the transformation of microtubes at high temperature, polymer chains should rearrange through the rapid breakage of ion-pairs. Thus, transformation is more facile for the microtubes assembled with lower MW polyelectrolytes. This result is consistent with the recent study by Jang et al. They demonstrated the molecular weight dependence on the disintegration of spin-assisted weak polyelectrolyte multilayer films [37]. When the LbL films were exposed at pH 2, the films assembled with lower MW disintegrated more rapidly. Based on the structural and chemical analysis, it was proposed that fast disintegration was due to the lower number of ion-pairing per single chain.

Although the microtubes assembled with low MW PAH and PAA at pH 5.5/5.5 were fairly stable in an aqueous solution, the microtubes became unstable when the $CaCl_2$ was added to the assembly solution (Fig. 3(b) vs. Fig. 5(a)). When multivalent ions are added in a polyelectrolyte solution, the polyelectrolyte becomes coiled due to the ion-bridging effect. Recently, it was demonstrated through cross-sectional imaging that LbL films of PAH and PSS exhibited a stratified film structure when divalent anions were added to the PAH assembly solution owing to the coiling of PAH [38]. Thus, when multivalent cations, $CaCl_2$, are added in our PAH/PAA LbL assembly, interdiffusion is frustrated because of the coiling of PAA, and ion-pairing decreases due to an ion-bridging effect. The microtubes become unstable due to the effect of multivalent ions coupled with lower MW polyelectrolytes, as described before. However, as the MW's of PAH (160,000 g/mol) and PAA (100,000 g/mol) increase, the microtubes become fairly stable in water despite the added $CaCl_2$. It is plausible that chain entanglements or a higher number of ion-pairs play an important role in the LbL film for high MW polymers.

As shown in Fig. 7, the aspect ratio of length and diameter of the microtubes decreased linearly with the incubation temperature. According to the previous studies, the T_g of PAH/PAA microtubes assembled at pH 7.5/3.5 was about 70 °C with 18 wt% of water as measured using MDSC. We should have observed the transition around this temperature in the plot of aspect ratio against incubation temperature. However, T_{tr} of LbL film with excess water, which is the condition for thermal incubation, could be different. For example, Zhang et al. showed that the T_{tr} of PAH/PAA polymer complex decreased about 50 °C as the water content increased 9 wt%, as measured by MDSC [26]. Thus, it is possible that the T_{tr} of PAH/PAA LbL films at excess water would be much lower than 70 °C, and the incubation temperature range is above the T_{tr} of PAH/PAA LbL film. However, thermal transition measurement of LbL films by MDSC is sensitive to only a limited range of water content, which deters the measurement in higher water content. T_{tr} in excess water can be measured using different techniques such as QCM-D, but this technique measures T_{tr} of LbL films supported on the substrate, which is thought to be different from the freestanding structured LbL assemblies [21]. More sophisticated studies are required for the study of thermal transitions in water.

CONCLUSION

The morphology and temperature-triggered transformation of the PAH/PAA LbL microtubes were studied varying assembly pH, MW, and added divalent salt. The microtubes prepared at pH 7.5/3.5 showed smoother surface morphology without perforation and transformed more easily compared to the microtubes assembled at pH 5.5/5.5. Also, the effectiveness of the thermal transformation was influenced by the MW and the number of LPs. Interestingly, the dimensional stability of the microtubes degraded when low MW PAH and PAA were used or when $CaCl_2$ was added. These results collectively indicate that the morphology and the transformation of LbL microtubes are closely associated with internal structure of the LbL films that is tuned by assembly pH, polymer MW, and added salt.

ACKNOWLEDGEMENT

This work was supported by Dong-Eui University Grant (201702680001).

REFERENCES

1. G. Decher, *Science*, **277**, 1232 (1997).
2. R. von Klitzing, *Phys. Chem. Chem. Phys.*, **8**, 5012 (2006).
3. P. Lavalle, J. C. Voegel, D. Vautier, B. Senger, P. Schaaf and V. Ball, *Adv. Mater.*, **23**, 1191 (2011).
4. S. Srivastava and N. A. Kotov, *Acc. Chem. Res.*, **41**, 1831 (2008).
5. N. Malikova, I. Pastoriza-Santos, M. Schierhorn, N. A. Kotov and L. M. Liz-Marzan, *Langmuir*, **18**, 3694 (2002).
6. A. P. R. Johnston, C. Cortez, A. S. Angelatos and F. Caruso, *Curr. Opin. Colloid Interface Sci.*, **11**, 203 (2006).
7. O. Azzaroni and K. H. A. Lau, *Soft Matter*, **7**, 8709 (2011).
8. Y. Wang, A. S. Angelatos and F. Caruso, *Chem. Mater.*, **20**, 848 (2008).
9. S. De Koker, R. Hoogenboom and B. G. De Geest, *Chem. Soc. Rev.*, **41**, 2867 (2012).
10. W. J. Tong, X. X. Song and C. Y. Gao, *Chem. Soc. Rev.*, **41**, 6103 (2012).
11. C. Y. Gao, S. Leporatti, S. Moya, E. Donath and H. Mohwald, *Chem. Eur. J.*, **9**, 915 (2003).
12. K. Kohler, D. G. Shchukin, H. Mohwald and G. B. Sukhorukov, *J. Phys. Chem. B*, **109**, 18250 (2005).
13. K. Koehler, H. Moehwald and G. B. Sukhorukov, *J. Phys. Chem. B*, **110**, 24002 (2006).
14. K. Kohler and G. B. Sukhorukov, *Adv. Funct. Mater.*, **17**, 2053 (2007).
15. W. J. Tong, S. P. She, L. L. Xie and C. Y. Gao, *Soft Matter*, **7**, 8258 (2011).
16. S. Leporatti, C. Gao, A. Voigt, E. Donath and H. Mohwald, *Eur. Phys. J. E*, **5**, 13 (2001).
17. K. Kohler, D. G. Shchukin, G. B. Sukhorukov and H. Mohwald, *Macromolecules*, **37**, 9546 (2004).
18. A. V. Dubrovskii, L. I. Shabarchina, Y. A. Kim and B. I. Sukhorukov, *Russ. J. Phys. Chem.*, **80**, 1703 (2006).
19. L. Shao and J. L. Lutkenhaus, *Soft Matter*, **6**, 3363 (2010).
20. B. Fortier-McGill and L. Reven, *Macromolecules*, **42**, 247 (2009).
21. A. Vidyasagar, C. Sung, R. Gamble and J. L. Lutkenhaus, *ACS Nano*, **6**, 6174 (2012).

22. A. Vidyasagar, C. Sung, K. Losensky and J. L. Lutkenhaus, *Macromolecules*, **45**, 9169 (2012).
23. C. H. Sung, K. L. Hearn and J. Lutkenhaus, *Soft Matter*, **10**, 6467 (2014).
24. E. Yildirim, Y. Zhang, J. L. Lutkenhaus and M. Sammalkorpi, *ACS Macro Lett.*, **4**, 1017 (2015).
25. R. Zhang, Y. P. Zhang, H. S. Antila, J. L. Lutkenhaus and M. Sammalkorpi, *J. Phys. Chem. B*, **121**, 322 (2017).
26. Y. P. Zhang, F. Li, L. D. Valenzuela, M. Sammalkorpi and J. L. Lutkenhaus, *Macromolecules*, **49**, 7563 (2016).
27. Q. He, W. Song, H. Moehwald and J. Li, *Langmuir*, **24**, 5508 (2008).
28. C. Sung, A. Vidyasagar, K. Hearn and J. L. Lutkenhaus, *J. Mater. Chem. B*, **2**, 2088 (2014).
29. S. Liu, K. Ghosh and M. Muthukumar, *J. Chem. Phys.*, **119**, 1813 (2003).
30. Y. Cho, W. Lee, Y. K. Jhon, J. Genzer and K. Char, *Small*, **6**, 2683 (2010).
31. S. S. Shiratori and M. F. Rubner, *Macromolecules*, **33**, 4213 (2000).
32. J. Choi and M. F. Rubner, *Macromolecules*, **38**, 116 (2005).
33. X. M. Liu, K. K. Goli, J. Genzer and O. J. Rojas, *Langmuir*, **27**, 4541 (2011).
34. S. Schlitt, A. Greiner and J. H. Wendorff, *Macromolecules*, **41**, 3228 (2008).
35. J. T. Chen, M. F. Zhang and T. P. Russell, *Nano Lett.*, **7**, 183 (2007).
36. J. D. Mendelsohn, C. J. Barrett, V. V. Chan, A. J. Pal, A. M. Mayes and M. F. Rubner, *Langmuir*, **16**, 5017 (2000).
37. Y. Jang, J. Seo, B. Akgun, S. Satija and K. Char, *Macromolecules*, **46**, 4580 (2013).
38. W. J. Dressick, K. J. Wahl, N. D. Bassim, R. M. Stroud and D. Y. Petrovykh, *Langmuir*, **28**, 15831 (2012).